HHS Public Access

Author manuscript

ACS Appl Mater Interfaces. Author manuscript; available in PMC 2017 May 25.

Published in final edited form as:

ACS Appl Mater Interfaces. 2016 May 25; 8(20): 12711–12719. doi:10.1021/acsami.6b03505.

Acidic pH-Triggered Drug-Eluting Nanocomposites for Magnetic Resonance Imaging-Monitored Intra-arterial Drug Delivery to Hepatocellular Carcinoma

Wooram Park[†], **Jeane Chen**[†], **Soojeong Cho**[†], **Sin-jung Park**[‡,⊥], **Andrew C. Larson**[†,§,‖], **Kun Na**[‡], and **Dong-Hyun Kim**[†,§]

Andrew C. Larson: a-larson@northwestern.edu; Kun Na: kna6997@catholic.ac.kr; Dong-Hyun Kim: dhkim@northwestern.edu

[†]Department of Radiology, Northwestern University Feinberg School of Medicine, Chicago, Illinois 60611, United States

[‡]Center for Photomedicine, Department of Biotechnology, The Catholic University of Korea, Bucheon-si, Gyeonggi do 14662, Republic of Korea

[§]Robert H. Lurie Comprehensive Cancer Center, Chicago, Illinois 60611, United States

[‖]Department of Biomedical Engineering, Department of Electrical Engineering and Computer Science, and International Institute of Nanotechnology, Northwestern University, Evanston, Illinois 60208, United States

Abstract

Transcatheter hepatic intra-arterial (IA) injection has been considered as an effective targeted delivery technique for hepatocellular carcinoma (HCC). Recently, drug-eluting beads (DEB) were developed for transcatheter IA delivery to HCC. However, the conventional DEB has offered relatively modest survival benefits. It can be difficult to control drug loading/release from DEB and to monitor selective delivery to the targeted tumors. Embolized DEBs in hepatic arteries frequently induce hypoxic and low pH conditions, promoting cancer cell growth. In this study, an acidic pH-triggered drug-eluting nanocomposite (pH-DEN) including superparamagnetic iron oxide nanocubes and pH-responsive synthetic peptides with lipid tails [octadecylamine–p(API-L-Asp)$_{10}$] was developed for magnetic resonance imaging (MRI)-monitored transcatheter delivery of sorafenib (the only FDA-approved systemic therapy for liver cancer) to HCC. The synthesized

Correspondence to: Andrew C. Larson, a-larson@northwestern.edu; Kun Na, kna6997@catholic.ac.kr; Dong-Hyun Kim, dhkim@northwestern.edu.

[⊥]Present Address

(S.-j.P.) Department of Biopharmaceutical Sciences, College of Pharmacy, University of Illinois, Chicago, IL 60612.

Supporting Information

The Supporting Information is available free of charge on the ACS Publications website at DOI: 10.1021/acsami.6b03505.

Eleven figures showing additional characterization data for pH-ADT and IONCs, high-magnification SEM image of pH-DENs, in vitro cell viability tests, and surgical procedure protocol for hepatic IA catheterization of pH-DENs in an orthotopic HCC rat model (PDF)

Author Contributions

The manuscript was written through contributions from all authors. All authors have given approval to the final version of the manuscript.

Notes

The authors declare no competing financial interest.

sorafenib-loaded pH-DENs exhibited distinct pH-triggered drug release behavior at acidic pH levels and highly sensitive MR contrast effects. In an orthotopic HCC rat model, successful hepatic IA delivery and distribution of sorafenib-loaded pH-DEN was confirmed with MRI. IA-delivered sorafenib-loaded pH-DENs elicited significant tumor growth inhibition in a rodent HCC model. These results indicate that the sorafenib–pH-DENs platform has the potential to be used as an advanced tool for liver-directed IA treatment of unresectable HCC.

Graphical Abstract

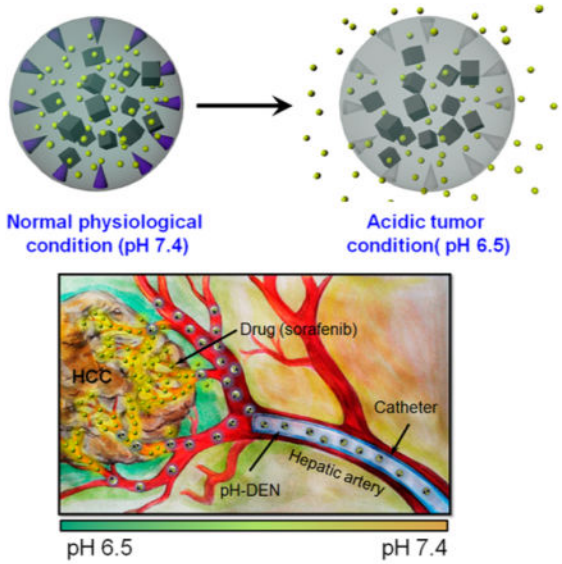

Keywords

nanocomposite microspheres; iron oxide nanoparticles; pH-responsive materials; hepatocellular carcinoma; sorafenib; image-guided therapy

INTRODUCTION

Hepatocellular carcinoma (HCC) is the sixth most prevalent cancer and the third leading cause of cancer-related deaths worldwide.[1,2] Resection and transplantation are the sole curative treatments for HCC, but only 10–15% of patients are candidates.[3] Systemic chemotherapy offers limited survival benefit, and regional minimally invasive therapies including thermal and chemical ablation have limited efficacy for the treatment of multifocal HCC.[4–6] Other promising treatment options are catheter-directed therapies such as transcatheter arterial chemoembolization (TACE), transcatheter arterial embolization (TAE), and ^{90}Y radioembolization. TACE, which involves intra-arterial (IA) infusion of embolic materials and chemotherapeutics, has been practiced in HCC patients for over 30 years.[7] The main purpose of TACE is to deliver a high dose of drug selectively to a tumor site while minimizing drug clearance.[7,8] Recently, drug-eluting beads (DEB) were developed for transcatheter IA drug delivery to HCC.[7,9,10] One of the most common DEB platforms in clinical use is composed of a nondegradable poly(vinyl alcohol) (PVA) microspheres that

can be loaded with doxorubicin by ionic interaction for liver-directed delivery. However, therapeutic efficacy of DEB–TACE has been limited by relatively rapid drug release and short retention in the targeted tumor tissues by first-order drug release from the beads.[7,11] Furthermore, visualization of DEB delivery to the tumors, either during or after an administration procedure, is not currently possible. The inability to monitor delivery and define procedural success during individual cases makes prediction of responses relatively difficult.

Stimuli- or environment-responsive strategies have recently emerged as the most promising approaches for selective drug delivery to tumor tissues.[12–14] These novel drug delivery systems are capable of controlling drug release behavior by responding to external stimuli such as pH, temperature, light, disease-specific enzymes, and magnetic field.[15–17] Among them, pH-sensitive drug carriers have been the most frequently used during targeted tumor therapy because pH is one of the features that clearly differentiates normal tissue from malignant tumor tissues in the body.[18,19] Generally, the extracellular region of solid tumors is acidic owing to excessive glycolysis and poor perfusion, referred to the “Warburg effect”.[20,21] In DEB–TACE procedures for liver cancers, the IA-infused DEBs induce insufficient blood flow in vessels and tumor by the embolic effect and lead to decreased pH by generating local hypoxic conditions and lactic acidosis.[22–25] Proton pumping from the hypoxic cells could facilitate the reduction of the surrounding pH.[26] Therefore, we hypothesized that a pH-triggered drug delivery system could be effective for local delivery of chemotherapeutic agents to liver tumor regions by TACE treatment (Figure 1b).

To this end, we developed pH-triggered drug-eluting nanocomposite microspheres (pH-DENs) for magnetic resonance imaging (MRI)-monitored transcatheter sorafenib drug delivery to HCC (Figure 1a,b). For the design of this system, biocompatible poly(lactide-*co*-glycolide) (PLGA) and synthesized iron oxide nanocubes (IONCs) were used as base materials for preparation of MRI-visible nanocomposites (NCs). While many image-guided approaches have been explored with PLGA microspheres,[27,28] MRI provides excellent soft tissue contrast and does not require exposure to ionizing radiation.[10,29] These NCs were loaded with the anti-angiogenic (AA) sorafenib multikinase inhibitor (Nexavar), the only U.S. Food and Drug Administration (FDA)-approved drug for treatment of advanced HCC. Sorafenib prevents angiogenesis via blockage of vascular endothelial growth factor (VEGF) and platelet-derived growth factor (PDGF) tyrosine receptors and cell proliferation via blockage of B-Raf and c-Raf of the mitogen-activated protein (MAP) kinase pathway.[30,31] However, the systemic administration of sorafenib following oral intake may not be acceptable to elicit consistently potent therapeutic responses.[10] Systemic exposure and a lack of tumor specificity can lead to severe side effects.[32] For acidic-specific sorafenib release, pH-responsiveness was rendered to these NCs. pH-responsive additive (pH-ADT, Figure 1c) was synthesized through a facile two-step process combining ring-opening polymerization (ROP) and aminolysis reactions,[15,33,34] and then incorporated into the NCs. The pH-ADT can be formed as a stable solid state at a neutral pH (normal tissue, pH ~ 7.4). However, an acidic environment (<pH ~ 7.4)[22–25] destabilizes the pH-ADT due to ionization of imidazole functional groups, causing phase transition of the pH-ADT into a charged water-soluble form. The solubility change of the additive in response to the acidic tumor pH triggers drug release from pH-sensitive NCs (Figure 1a). We hypothesized that these newly

designed sorafenib-loaded pH-DENs can be selectively infused via targeted transcatheter MRI-monitored delivery to liver tumors and that pH-responsive sorafenib drug release from these pH-DENs would elicit significant tumor growth inhibition in an orthotopic rodent model of HCC (Figure 1b).

EXPERIMENTAL METHODS

Materials

All reagents and solvents were obtained commercially and used without further purification. Poly(D,L-lactide-*co*-glycolide) (lactide:glycolide 50:50, PLGA), poly(vinyl alcohol) (M_w 89 000–98 000, 99+% hydrolyzed, PVA), *β*-benzyl-L-aspartate (BLA), 1-(3-aminopropyl)imidazole (API), octadecylamine, iron(III) chloride hexahydrate (≥98%), *N*,*N*-dimethylformamide (DMF), tetrahydrofuran (THF), diethyl ether (≥99.9%), dichloromethane (CH_2Cl_2), chloroform ($CHCl_3$), dimethyl sulfoxide (DMSO), methanol, *n*-docosane (99%), 1-octadecene (90%), *n*-hexane, and ethanol were purchased from Sigma–Aldrich Co (Milwaukee, WI). Sodium oleate (>97%) and triphosgene (98%) were purchased from TCI America (Portland, OR). Sorafenib tosylate was purchased from LC Laboratories (Woburn, MA). Iron oleate was prepared by following a reported procedure.[35] *β*-Benzyl-L-aspartate *N*-carboxy anhydride (BLA-NCA) was synthesized by following our previous report.[15,33]

Synthesis of Iron Oxide Nanocubes

IONCs were synthesized by thermal decomposition of iron(III) oleate in the presence of sodium oleate, according to a modified literature procedure.[36,37] As-prepared iron oleate (1.57 g, 1.75 mmol), *n*-docosane (6.0 g, 19.32 mmol), and sodium oleate (0.53 g, 1.74 mmol) were mixed with 11 mL of 1-octadecene in a 50 mL three-neck round-bottom flask. The reaction mixture was heated to 120 °C under high vacuum and stirred for 1 h. The reaction mixture was then heated to 337 °C with a heating rate of 3 °C/min under nitrogen atmosphere and stirred at this temperature for 30 min. Then the reaction mixture was cooled to 80°C. IONCs were precipitated in a mixture composed of 2 volumes of *n*-hexane and 3 volumes of ethanol (with respect to the original solution volume). The supernatant was discarded and the precipitates were redispersed in *n*-hexane and washed with ethanol. The washing process was repeated three times. Finally, the IONCs were dried under vacuum and redispersed in chloroform.

Synthesis of pH-Sensitive Additive

pH-ADT was synthesized on the basis of our previously reported procedure.[33] Octadecylamine (0.3 g 1.2 mmol) was dissolved in a mixture of DMF (10 mL) and CH_2Cl_2 (50 mL) and then stirred at room temperature for 2 h. As-synthesized BLA-NCA (3 g, 12 mmol) was dissolved in DMF (10 mL) and dropped into the octadecylamine solution. The reaction mixture was stirred for 2 days. To remove CH_2Cl_2, the reaction solution was concentrated in a rotary evaporator for 30 min under vacuum. The final product was precipitated in diethyl ether (200 mL) and collected by centrifugation (3500 rpm) for 5 min. This process repeated three times to remove any unreacted impurity. The precipitate was dried under vacuum at room temperature. Finally, pH-ADT [octadecylamine–p(API-Asp)$_{10}$]

was synthesized via aminolysis of the octadecylamine–polyBLA with API, following our previous report.[15,33] As-synthesized octadecylamine–p(BLA)$_{10}$ (0.2 g, 74.8 μmol) was dissolved in DMF (5 mL). API (1 g, 7.9 mmol) was added to the octadecylamine–p(BLA)$_{10}$ solution, which was stirred for 12 h at room temperature. After 12 h, the reaction mixture was added dropwise into a cooled aqueous solution of 0.1 N HCl (20 mL) to neutralize the reaction mixture. To remove any impurity, the solution was dialyzed by use of a cellulose membrane [molecular weight cutoff (MWCO) 1000, Spectrum Laboratories, Rancho Dominguez, CA] against 0.01 N HCl solution three times. The final solution was lyophilized and octadecylamine–p(API-L-Asp)$_{10}$ was obtained as a white solid. The chemical structure of the synthesized polymer was determined by ^{1}H NMR. ^{1}H NMR spectra were recorded in DMSO-d_6 at room temperature on a Bruker NMR spectrometer at 500 MHz.

Morphology and Size Analysis of Iron Oxide Nanocubes

IONCs were monitored by transmission electron microscopy (TEM; FEI Tecnai Spirit G2, Hillsboro, OR) operating at 120 kV.

Preparation of pH-Triggered Drug-Eluting Nanocomposites

pH-DENs were manufactured via the emulsion/solvent evaporation method.[38,39] PLGA (100 mg) was dissolved in 4 mL of CH_2Cl_2 and then combined with 20 mg of sorafenib dissolved in 200 μL of DMSO, 1 mg of oleic acid-stabilized IONCs dissolved in 100 μL of CH_2Cl_2, and 10 mg of pH-ADT dissolved in 100 μL of methanol. The solution was mixed by vortexing for 1 min. This primary emulsion was further dropped into PVA (2 wt %) solution to form an emulsion by use of a homogenizer (300D Disital benchtop homogenizer, VWR) at 2000 rpm for 5 min. The emulsion was stirred for 12 h under overhead stirring (200 rpm) at room temperature. The PLGA microspheres were centrifuged for 5 min at 3000 rpm and then washed three times with deionized water. The resulting pH-DENs were lyophilized and stored at −20 °C. The morphology and size distribution of the pH-DENs were observed by scanning electron microscopy (SEM; Hitachi S-4800, Hitachi, Japan).

Characterization of Sorafenib Loaded in pH-Triggered Drug-Eluting Nanocomposites

Sorafenib content in pH-DENs was analyzed by high performance liquid chromatography (HPLC), as in a previous report.[40] pH-DENs (30 mg) were dissolved in 1 mL of a solution of 1% DMSO in a mixture of acetonitrile and ammonium acetate (60:40 v/v). The polymer and IONCs were collected by centrifugation (15 000 rpm, 5 min). The supernatant was analyzed for sorafenib concentration on an Agilent 1260 Infinity Quaternary LC HPLC system (Santa Clara, CA) equipped with a Zorbax C18 column (Agilent, 5 μm, 9.4 × 250 mm).

Characterization of Iron Oxide Nanocubes Loaded in pH-Triggered Drug-Eluting Nanocomposites

The IONCs (Fe) content in pH-DENs was characterized by inductively coupled plasma mass spectrometry (ICP-MS, PerkinElmer, Waltham, MA). In triplicate, pH-DEN (10 mg) were digested in 200 μL of nitric acid (70%) at 60 °C and diluted to 5 mL of a 2% nitric acid solution with 5 parts per billion (ppb) yttrium as an internal standard.

Characterization of Magnetic Properties of Iron Oxide Nanocubes

The hysteresis loop of IONC was analyzed on an MPMS XL-7 superconducting quantum interference device (SQUID) magnetometer (Quantum Design, San Diego, CA) at 300 K. The result was normalized with the grams of iron (Fe) quantified by ICP optical emission spectroscopy (OES) in each sample.

Characterization of T_2 Relaxivity Properties

Quantitative R_2 relaxivity measurements were performed by use of a 7 T MRI scanner (BioSpec, Bruker, Billerica, MA). Imaging phantoms were prepared by using 1% agar phantoms at various different concentrations of pH-DENs (0–20 mg/mL). These phantom studies were performed as per our previous report.[10] A Carr–Purcell–Meiboom–Gill (CPMG) sequence (TR (repetition time) = 1s, 1 mm slice thickness, 6 TE (echo time) ranging from 10 to 60 ms) was applied with a 7 T MRI scanner. R_2 time constants were determined by fitting signal decay curves to the monoexponential function $S(\mathrm{TE}) = M_0 e^{-\mathrm{TE}/T_2}$. The Pearson correlation coefficient was calculated between the iron concentration and resultant R_2 values. The slope of the resulting linear least-squares fit line provided the R_2 relaxivity in units of $s^{-1}.mM^{-1}$.

In Vitro Drug Release Test

pH-DENs or non-pH-DENs (30 mg) were incubated in 5 mL of 10 mM phosphate-buffered saline (PBS; pH 7.4 or 6.5, with 0.02 wt % Tween 80) at 37 °C with continuous agitation at 50 rpm. At predetermined time points, the release medium was collected and replaced with fresh release medium. To determine the released sorafenib, HPLC analysis was performed as mentioned above.

In Vitro Cytotoxicity Test

McA-RH7777 hepatoma cells were obtained from ATCC (Manassas, VA) and cultured in Dulbecco's modified Eagle's medium (DMEM) containing 10% fetal bovine serum (Sigma–Aldrich, St. Louis, MO). The cells were cultured at 37°C with 5% CO_2, and the culture medium was replaced with fresh medium every 2–3 days. After preculture for 7 days, the cells were seeded in 6-well plates at a density of 2.5×10^5 cells/well and incubated for 24 h. The culture medium was replaced with pH-DENs or non-pH-DENs containing DMEM medium (equivalent to sorafenib dose of 10 μg/mL) and incubated at pH 7.4 or 6.5 for 48 h. As a control group, the cells were treated with 0.5 mL of DMEM under the same conditions. To determine cell viability, cell counting kit 8 (CCK-8, Dojindo Molecular Technologies, Gaithersburg, MD) assay was performed according to the manufacturers' instructions.

In Vivo Orthotopic Hepatocellular Carcinoma Rat Model

Studies were performed with approval from the Institutional Animal Care and Use Committee (IACUC) at Northwestern University. In vivo orthotopic HCC rat model was established with MCA-RH7777 hepatoma cells, following our previous report.[10] These animal models were divided into two groups: an untreated control group (three rats) and a group treated with pH-DENs (three rats).

Catheterization Procedures

The rats treated with pH-DENs underwent procedures to invasively catheterize the proper hepatic artery (Figure S8, Supporting Information), as described in our previous reports.[10,41] A 20 mg dose of the pH-DENs (equivalent to sorafenib dose of 9.3 mg/kg) was administrated through hepatic IA route. In the comparison group, PBS was administered to the animals under the same conditions.

In Vivo Magnetic Resonance Imaging of pH-Triggered Drug-Eluting Nanocomposite Delivery to Liver Tumors

T_2-weighted images were collected pre- and postcatheterization and IA infusion of the pH-DEN, as described above. MR scans were performed in both coronal and axial orientations using a gradient-echo sequence with the following parameters: TR/T_E = 1136/28 ms, 1 mm slice thickness, field of view (FOV) 71 × 85 mm, 216 × 256 matrix, and respiratory triggering with a MRI-compatible small-animal gating system (model 1025, SA Instruments, Stony Brook, NY).

Tumor Size Measurement

The width (a) and length (b) of the tumors were measured MRI every other day posttreatment. Tumor volume (V) was calculated as $V = a^2b/2$ (where a is width, b is length, and $a \leq b$). For comparison purposes, the tumor volume was normalized by its initial volume as V/V_0 (V_0 was the volume of the tumor at the time that catheterization and pH-DEN infusion was performed).

Histology and Immunohistochemistry

To confirm the antitumor therapeutic efficacy of pH-DENs, the livers were harvested from the rat 7 days postinfusion. Harvested tissue was sectioned with 5μm thickness and stained with hematoxylin and eosin (H/E) and rat anti-CD34, respectively. To assess delivery of IONC-containing pH-DENs to HCC, livers were harvested from the rats 24 h postinfusion (n = 3 rats) and Prussian blue staining was performed on slices of formalin-fixed tissues. All slides were analyzed on a TissueFAXS microscope (TissueGnostics GmbH, Vienna, Austria).

Statistical Analysis

Data are expressed as mean ± standard deviation (SD) or standard error (SE). Differences between the values were assessed by Student's t-test.

RESULTS AND DISCUSSION

Synthesis of pH-Responsive Additive and Iron Oxide Nanocubes

pH-ADT was synthesized by combining the ROP of β-benzyl-L-aspartate N-carboxyanhydride (BLA-NCA) and an aminolysis reaction (Figure 2a) as per our previous report.[33] Successful synthesis of ionizable imidazole-functionalized polypeptide with octadecylamine tail was confirmed by ^{1}H NMR analysis (Figure 2b). The degree of polymerization (DP) of imidazole-functionalized L-aspartate units was determined to be 10.

The pH sensitivity of pH-ADT was characterized by light transmittance of pH-ADT solution in water (Figure 2c). Transmittance of pH-ADT solution dropped sharply over the narrow pH range of 6.5–7.0 upon acid titration from pH 8.0 to 3.0. It should be noted that the pH-dependent phase transition behavior of the pH-ADT was completely reversible when the pH was cycled between 7.4 and 6.5 (Figure S1, Supporting Information), suggesting a highly sensitive response to the environmental pH value. Iron oxide nanocubes (IONCs) were synthesized via thermal decomposition of iron–oleate complex in a mixture composed of sodium oleate, *n*-docosane, and 1-octadecene, as described in a previous report.[35–37] A transmission electron microscopy (TEM) image shows that monodisperse cube-shaped nanoparticles were obtained with an average size of 24 ± 2.0 nm (Figure 2d; Figures S2 and S3, Supporting Information). At 300 K, these iron oxide nanocubes exhibited superparamagnetic behavior with no coercivity or remanence and a measured saturation magnetization (M_S) of ~50 emu/gFe (Figure 2e).

Preparation of pH-Triggered Drug-Eluting Nanocomposites and Their Physicochemical Characterization

pH-DENs were prepared by the double-emulsion method.[38–40] Hydrophobic sorafenib and IONCs were coencapsulated in pH-ADT-embedded PLGA microspheres (pH-DENs; Table 1). Scanning electron microscope (SEM) images showed that pH-DENs exhibited smooth and uniform spherical morphology with size of 5 ± 1.5 μm (Figure 3a,b; Figure S4, Supporting Information). Co-embedding the pH-ADT and sorafenib in PLGA microspheres resulted in significantly enhanced drug-loading efficiency (approximately 20% increase), which is attributed to the hydrophobic interaction between hydrophobic drug (i.e., sorafenib) and lipid tail of pH-ADT (Table 1). The magnetic property of pH-DENs was confirmed by their separation within 30 min in the presence of a magnetic field (500 G permanent magnet) (Figure 3c). To demonstrate MR contrast effect of pH-DEN, a concentration-dependent signal decay was observed in T_2-weighted MR images and R_2 relaxivity value of pH-DEN was determined to be 1595 $mM^{-1}.s^{-1}$ (in agar phantom at field strength of 7 T at 300 K) (Figure 3d); the latter result suggested the feasibility of using MRI to monitor in vivo delivery of our pH-DEN drug delivery carriers.

Acidic pH Responsiveness of pH-Triggered Drug-Eluting Nanocomposites

In the PLGA-based polymeric drug delivery system, diffusion and degradation/erosion were known as primary mechanisms of drug release.[42,43] In this regard, we hypothesized that the pH-dependent phase transition behavior of pH-ADT in the pH-DENs could facilitate the degradation/erosion of polymer matrix in acid microenvironments, resulting in fast release of sorafenib. To demonstrate the pH-induced drug release behavior, sorafenib release profiles from the pH-DENs were investigated at both the physiological pH of 7.4 and the acidic tumor microenvironment pH of 6.5 (Figure 4a).[19] As we expected, the pH-DENs exhibited significantly increased drug release rate at pH 6.5 (cumulative drug release amount ~80% at 96 h), whereas the amount of sorafenib released from pH-DEN at pH 7.4 was markedly reduced (cumulative drug release amount ~50% at 96 h). In this study, non-pH-responsive DENs (non-pH-DEN, Table 1) composed of PLGA, sorafenib, and IONCs without pH-ADT were used as a control group. Non-pH-DENs showed only a slight increase in drug release rate at acidic conditions compared to that at normal conditions; this may be

caused by acid-accelerated hydrolysis of the PLGA polymer.[44] These results indicate that the combined effect of phase transition of pH-ADT and accelerated hydrolysis of PLGA at acidic pH can trigger rapid sorafenib release from these pH-DENs. The cytotoxicity of the sorafenib-loaded pH-DENs was evaluated in McA-RH7777 hepatoma cells at pH 7.4 and 6.5 by use of a cell counting kit 8 assay (Figure 4b). Before the experiment, the influence of acidic pH on cell viability was confirmed in McA-RH7777 hepatoma cells. No difference in viability was observed between normal and acidic pH conditions (Figure S5, Supporting Information), which indicates that the acidic pH condition does not affect cell viability. As shown in Figure 4b, above a treatment concentration of 50 μg/mL, sorafenib–pH-DENs significantly enhanced cytotoxicity at pH 6.5 compared to the treated cells at pH 7.4 ($*p < 0.01$), whereas the sorafenib–non-pH-DENs exhibited no difference between pH 6.5 and 7.4 conditions (Figure S6, Supporting Information). Cell viability tests at different pH conditions were also performed with normal liver (clone 9) cells as a comparison group. The results showed a similar trend as that against HCC tumor cells, which indicates that the therapeutic effect of pH-DENs was mainly influenced by the acidic extracellular environment, regardless of cell type (Figure S7, Supporting Information). Since the extracellular pH value of healthy liver tissue was known to be neutral due to their strict pH homeostasis,[45,46] under in vivo conditions, the cytotoxicity of pH-DEN could be significantly reduced in normal liver tissues. Taken all together, these results demonstrate that the triggered sorafenib release of the pH-DENs responding to acidic extracellular pH condition increased drug concentration in the culture medium and thus led to markedly enhanced therapeutic efficiency against HCC tumor cells.

Magnetic Resonance Imaging-Monitored Hepatic Intra-arterial Transcatheter Infusion of Sorafenib-Loaded pH-Triggered Drug-Eluting Nanocomposites in Orthotopic Hepatocellular Carcinoma Rat Model

To evaluate in vivo imaging capabilities and therapeutic effects of sorafenib–pH-DENs, we used an orthotopic HCC rat model. McA-RH7777 hepatoma cells were inoculated into Sprague-Dawley rats, and sorafenib–pH-DENs were infused via IA route after 1 week of tumor growth (dose of pH-DENs was 20 mg/rat). Catheterization procedures were successfully performed in each animal (Figure S8, Supporting Information). To visualize transcatheter delivery of sorafenib–pH-DENs to the tumors, we performed MR imaging on a 7 T MRI system. Tumors were visualized as hyperintense regions relative to the surrounding normal liver tissues in T_2-weighted images (Figure 5a, left panels). However, local signal reductions were observed in the tumor region immediately after transcatheter infusion of sorafenib–pH-DENs (Figure 5a, right panels), indicating efficient accumulation of pH-DENs exhibiting high R_2 relaxivity (Figure 3d) in the tumor site. MRI observation of sorafenib–pH-DENs deposition within the liver was later confirmed with histological staining of the tissue for iron with Prussian blue.[9,10] As shown in Figure 5b, strong blue signal was observed not only at the peripheral rim of the tumor (upper image) but also at the intratumor vessel (bottom image). These results indicate that sorafenib–pH-DENs were effectively localized to the targeted tumor regions, including the rim and inner tumor, via transcatheter IA liver-directed infusion.[41] The embolic pH-DENs in arteries diminish blood flow and induce low pH with hypoxia and lactic acidosis.[22–25] Additionally, acid-mediated tumor invasion processes results in significantly acidic pH environment in HCC tumors.[24,25] The

acidic HCC tumor environment that can trigger drug release could be confirmed with overexpression of pH-regulatory protein (hydrogen/potassium ATPase). Overexpression of hydrogen/potassium ATPase was seen in the peripheral rim and inner tumor regions around the vessels (Figure S9, Supporting Information). Taken together, the successful localization of pH-DEN in the tumor regions of peripheral rim and inner tumor could elicit the pH-triggered drug release response to the acidic microenvironment.

In Vivo Therapeutic Efficacy of Sorafenib-Loaded pH-Triggered Drug-Eluting Nanocomposites in Orthotopic Hepatocellular Carcinoma Rat Model

Therapeutic efficacy of IA-infused sorafenib–pH-DENs was determined by measuring tumor size as estimated from MRI images and physical examination of the excised liver. Then therapeutic outcomes were further evaluated via histological and immunohistochemical staining of the tumor tissues harvested during end-point necropsy (1 week after sorafenib–pH-DEN injection). Tumors treated with sorafenib–pH-DENs demonstrated significant growth inhibition (Figure 6a,b) compared to control group tumors (PBS-treated HCC rats). Histological analysis of the tumor tissues showed that HCC treated with sorafenib–pH-DENs markedly reduced the number of cancerous cells (H/E staining) and increased the number of terminal deoxynucleotidyl transferase dUTP nick end-labeling (TUNEL)-positive tumor cells in both the rim and center regions of HCC tumor [see region enclosed by yellow dotted line in the images, Figure 6c (middle)]. However, in the sorafenib–non-pH-DEN-treated group, the apoptosis rate in overall tumor tissues was significantly lower compared to the pH-DEN-treated group, and apoptotic cells were observed only at the peripheral rim of HCC tumor region (Figures S10 and S11, Supporting Information). This limited therapeutic outcome could be attributed to nontriggered slow drug release rate of non-pH-DENs. According to our previous report,[10] free sorafenib-treated HCC rat model also showed limited therapeutic efficacy. Taken together, these results indicate that the pH-triggered release of sorafenib from IA-targeted pH-DENs can efficiently inhibit proliferation and induce apoptosis against HCC tumor cells (Figure 6c). Anti-angiogenic effect of sorafenib, which is a major mechanism for control of tumor growth, was well demonstrated in the immunohistochemical staining for CD34.[31,47] As shown in Figure 6c (bottom), antiangiogenic effects were clearly observed in sorafenib–pH-DEN-treated tumors with qualitatively appreciable reductions in CD34 expression compared to control tumors. It is worth noting that the reduction of CD34 expression level was shown in a much broader region compared with that described in our previous report (which used pH-ins-NCs).[10] This result indicates that pH sensitivity could enhance the therapeutic efficacy of sorafenib in the HCC tumor region due to rapid drug release in the acidic tumor microenvironment during TACE procedures of HCC.[48,49]

CONCLUSIONS

In conclusion, a new acidic pH-triggered drug-eluting nanocomposite (pH-DEN) has been developed for the treatment of HCC; these pH-DENs are composed of biocompatible PLGA, iron oxide nanocubes (IONCs), and pH-responsive synthetic peptides with lipid tails. The synthesized pH-DENs exhibited pH-triggered drug release behavior at acidic pH levels as well as highly sensitive MR contrast effects. In an orthotopic HCC rat model, the pH-DENs

were successfully administered via selective transcatheter hepatic IA delivery to HCC, and the embolized pH-DENs around rim and inner tumors could be confirmed with MRI. Local pH-responsive sorafenib release from IA-infused sorafenib–pH-DENs into HCC demonstrated significant tumor growth inhibition with antiangiogenic effects. These outcomes indicate that this newly developed pH-DEN platform has the potential to be applied as an advanced new form of IA chemotherapy for treatment of unresectable HCC.

Supplementary Material

Refer to Web version on PubMed Central for supplementary material.

Acknowledgments

This work was supported by a Basic Research Grant from ACS (American Cancer Society, ACS 279148) and by four grants (R01CA141047, R21CA173491, R21EB017986, and R21CA185274) from the National Cancer Institute and National Institute of Biomedical Imaging and Bioengineering. This work was supported by the Center for Translational Imaging and Mouse Histology and Phenotyping Laboratory at Northwestern University. This work was supported by the Basic Research Laboratory (BRL) Program through a National Research Foundation of Korea (NRF) grant funded by the Korean government (MSIP) (2015R1A4A1042350). We are grateful to Alexandra I. Gaudette, Dr. Ie-Rang Jeon, and Dr. T. David Harris (Department of Chemistry, Northwestern University) for SQUID analysis.

References

1. Fujimoto A, Totoki Y, Abe T, Boroevich KA, Hosoda F, Nguyen HH, Aoki M, Hosono N, Kubo M, Miya F, et al. Whole-genome Sequencing of Liver Cancers Identifies Etiological Influences on Mutation Patterns and Recurrent Mutations in Chromatin Regulators. Nat Genet. 2012; 44:760–764. [PubMed: 22634756]
2. Forner A, Llovet JM, Bruix J. Hepatocellular Carcinoma. Lancet. 2012; 379:1245–1255. [PubMed: 22353262]
3. Poon RTP, Ngan H, Lo CM, Liu CL, Fan ST, Wong J. Transarterial Chemoembolization for Inoperable Hepatocellular Carcinoma and Postresection Intrahepatic Recurrence. J Surg Oncol. 2000; 73:109–114. [PubMed: 10694648]
4. Trinchet J-C, Ganne-Carrie N, Beaugrand M. Intra-arterial Chemoembolization in Patients with Hepatocellular Carcinoma. Hepato-gastroenterology. 1998; 45(Suppl 3):1242–1247. [PubMed: 9730382]
5. Salem R, Lewandowski RJ, Mulcahy MF, Riaz A, Ryu RK, Ibrahim S, Atassi B, Baker T, Gates V, Miller FH, et al. Radioembolization for Hepatocellular Carcinoma using Yttrium-90 Microspheres: a Comprehensive Report of Long-term Outcomes. Gastroenterology. 2010; 138:52–64. [PubMed: 19766639]
6. Abdelmaksoud MH, Hwang GL, Louie JD, Kothary N, Hofmann LV, Kuo WT, Hovsepian DM, Sze DY. Development of New Hepaticoenteric Collateral Pathways after Hepatic Arterial Skeletonization in Preparation for Yttrium-90 Radioembolization. J Vasc Interv Radiol. 2010; 21:1385–1395. [PubMed: 20688531]
7. Lewis AL, Dreher MR. Locoregional Drug Delivery Using Image-guided Intra-Arterial Drug Eluting Bead Therapy. J Controlled Release. 2012; 161:338–350.
8. Lewandowski RJ, Geschwind JF, Liapi E, Salem R. Transcatheter Intraarterial Therapies: Rationale and Overview. Radiology. 2011; 259:641–657. [PubMed: 21602502]
9. Kim DH, Chen J, Omary RA, Larson AC. MRI Visible Drug Eluting Magnetic Microspheres for Transcatheter Intra-Arterial Delivery to Liver Tumors. Theranostics. 2015; 5:477. [PubMed: 25767615]
10. Chen J, Sheu AY, Li W, Zhang Z, Kim DH, Lewandowski RJ, Omary RA, Shea LD, Larson AC. Poly (lactide-co-glycolide) Microspheres for MRI-monitored Transcatheter Delivery of Sorafenib to Liver Tumors. J Controlled Release. 2014; 184:10–17.

11. Kettenbach J, Stadler A, Katzler Iv, Schernthaner R, Blum M, Lammer J, Rand T. Drug-loaded Microspheres for the Treatment of Liver Cancer: Review of Current Results. Cardiovascular Intervent Radiol. 2008; 31:468–476.
12. Park W, Na K. Advances in the Synthesis and Application of Nanoparticles for Drug Delivery. Wiley Interdiscip Rev: Nanomed Nanobiotechnol. 2015; 7:494–508. [PubMed: 25583540]
13. Mura S, Nicolas J, Couvreur P. Stimuli-esponsive Nano-carriers for Drug Delivery. Nat Mater. 2013; 12:991–1003. [PubMed: 24150417]
14. Lee D, Hong JW, Park C, Lee H, Lee JE, Hyeon T, Paik SR. Ca^{2+}-Dependent Intracellular Drug Delivery System Developed with “Raspberry-Type” Particles-on-a-Particle Comprising Mesoporous Silica Core and α-Synuclein-Coated Gold Nanoparticles. ACS Nano. 2014; 8:8887–8895. [PubMed: 25166911]
15. Ling D, Park W, Park S-j, Lu Y, Kim KS, Hackett MJ, Kim BH, Yim H, Jeon YS, Na K, Hyeon T. Multifunctional Tumor pH-sensitive Self-assembled Nanoparticles for Bimodal Imaging and Treatment of Resistant Heterogeneous Tumors. J Am Chem Soc. 2014; 136:5647–5655. [PubMed: 24689550]
16. Lee CS, Park W, Park S-j, Na K. Endolysosomal Environment-responsive Photodynamic Nanocarrier to Enhance Cytosolic Drug Delivery via Photosensitizer-mediated Membrane Disruption. Biomaterials. 2013; 34:9227–9236. [PubMed: 24008035]
17. Kim DH, Guo Y, Zhang Z, Procissi D, Nicolai J, Omary RA, Larson AC. Temperature-Sensitive Magnetic Drug Carriers for Concurrent Gemcitabine Chemohyperthermia. Adv Healthcare Mater. 2014; 3:714–724.
18. Schornack PA, Gillies RJ. Contributions of Cell Metabolism and H^+ Diffusion to the Acidic pH of Tumors. Neoplasia. 2003; 5:135–145. [PubMed: 12659686]
19. Tannock IF, Rotin D. Acid pH in Tumors and Its Potential for Therapeutic Exploitation. Cancer Res. 1989; 49:4373–4384. [PubMed: 2545340]
20. Gatenby RA, Gillies RJ. Why Do Cancers Have High Aerobic Glycolysis? Nat Rev Cancer. 2004; 4:891–899. [PubMed: 15516961]
21. Song J, Ge Z, Yang X, Luo Q, Wang C, You H, Ge T, Deng Y, Lin H, Cui Y, et al. Hepatic Stellate Cells Activated by Acidic Tumor Microenvironment Promote the Metastasis of Hepatocellular Carcinoma via Osteopontin. Cancer Lett. 2015; 356:713–720. [PubMed: 25449435]
22. Robergs RA, Ghiasvand F, Parker D. Biochemistry of Exercise-induced Metabolic Acidosis. Am J Physiol: Regul, Integr Comp Physiol. 2004; 287:R502–R516. [PubMed: 15308499]
23. Stuart K. Chemoembolization in the Management of Liver Tumors. Oncologist. 2003; 8:425–37. [PubMed: 14530495]
24. Gatenby RA, Gawlinski ET, Gmitro AF, Kaylor B, Gillies RJ. Acid-mediated Tumor Invasion: a Multidisciplinary Study. Cancer Res. 2006; 66:5216–5223. [PubMed: 16707446]
25. Robey IF, Baggett BK, Kirkpatrick ND, Roe DJ, Dosescu J, Sloane BF, Hashim AI, Morse DL, Raghunand N, Gatenby RA, Gillies RJ. Bicarbonate Increases Tumor pH and Inhibits Spontaneous Metastases. Cancer Res. 2009; 69:2260–2268. [PubMed: 19276390]
26. Vooijs MA, Gort EH, Groot AJ, van der Wall E, van Diest PJ. Hypoxic Regulation of Metastasis via Hypoxia-inducible Factors. Curr Mol Med. 2008; 8:60–67. [PubMed: 18289014]
27. Kazazi-Hyseni F, Van Vuuren S, Van Der Giezen D, Pieters E, Ramazani F, Rodriguez S, Veldhuis G, Goldschmeding R, Van Nostrum C, Hennink W, Kok RJ. Release and Pharmacokinetics of Near-Infrared Labeled Albumin from Monodisperse Poly (d, l-lactic-co-hydroxymethyl glycolic acid) Microspheres after Subcapsular Renal Injection. Acta Biomater. 2015; 22:141–154. [PubMed: 25929814]
28. Chen J, White SB, Harris KR, Li W, Yap JW, Kim DH, Lewandowski RJ, Shea LD, Larson AC. Poly (lactide-co-glycolide) Microspheres for MRI-monitored Delivery of Sorafenib in a Rabbit VX2 Model. Biomaterials. 2015; 61:299–306. [PubMed: 26022791]
29. Li W, Zhang Z, Gordon AC, Chen J, Nicolai J, Lewandowski RJ, Omary RA, Larson AC. SPIO-labeled Yttrium Microspheres for MR Imaging Quantification of Transcatheter Intrahepatic Delivery in a Rodent Model. Radiology. 2016; 278:405–412. [PubMed: 26313619]

30. Wilhelm S, Carter C, Lynch M, Lowinger T, Dumas J, Smith RA, Schwartz B, Simantov R, Kelley S. Discovery and Development of Sorafenib: a Multikinase Inhibitor for Treating Cancer. Nat Rev Drug Discovery. 2006; 5:835–844. [PubMed: 17016424]
31. Llovet JM, Ricci S, Mazzaferro V, Hilgard P, Gane E, Blanc JF, de Oliveira AC, Santoro A, Raoul JL, Forner A, et al. Sorafenib in Advanced Hepatocellular Carcinoma. N Engl J Med. 2008; 359:378–390. [PubMed: 18650514]
32. Han G, Yang J, Shao G, Teng G, Wang M, Yang J, Liu Z, Feng G, Yang R, Lu L, Chao Y, Wang J. Sorafenib in Combination with Transarterial Chemoembolization in Chinese Patients with Hepatocellular Carcinoma: a Subgroup Interim Analysis of the START Trial. Future Oncol. 2013; 9:403–410. [PubMed: 23469975]
33. Ling D, Xia H, Park W, Hackett MJ, Song C, Na K, Hui KM, Hyeon T. pH-sensitive Nanoformulated Triptolide as a Targeted Therapeutic Strategy for Hepatocellular Carcinoma. ACS Nano. 2014; 8:8027–8039. [PubMed: 25093274]
34. Jeong S, Park W, Lee CS, Na K. A Cancer-Recognizing Polymeric Photosensitizer Based on the Tumor Extracellular pH Response of Conjugated Polymers for Targeted Cancer Photodynamic Therapy. Macromol Biosci. 2014; 14:1688–1695. [PubMed: 25251581]
35. Park J, An K, Hwang Y, Park JG, Noh HJ, Kim JY, Park JH, Hwang NM, Hyeon T. Ultra-large-scale Syntheses of Monodisperse Nanocrystals. Nat Mater. 2004; 3:891–895. [PubMed: 15568032]
36. Singh G, Chan H, Baskin A, Gelman E, Repnin N, Král P, Klajn R. Self-assembly of Magnetite Nanocubes into Helical Superstructures. Science. 2014; 345:1149–1153. [PubMed: 25061133]
37. Kovalenko MV, Bodnarchuk MI, Lechner RT, Hesser G, Schäffler F, Heiss W. Fatty Acid Salts as Stabilizers in Size-and Shape-Controlled Nanocrystal Synthesis: the Case of Inverse Spinel Iron Oxide. J Am Chem Soc. 2007; 129:6352–6353. [PubMed: 17472378]
38. Park W, Na K. Polyelectrolyte Complex of Chondroitin Sulfate and Peptide with Lower pI Value in Poly (lactide-co-glycolide) Microsphere for Stability and Controlled Release. Colloids Surf, B. 2009; 72:193–200.
39. Park W, Kim D, Kang HC, Bae YH, Na K. Multi-arm Histidine Copolymer for Controlled Release of Insulin from Poly (lactide-co-glycolide) Microsphere. Biomaterials. 2012; 33:8848–8857. [PubMed: 22959184]
40. Blanchet B, Billemont B, Cramard J, Benichou A, Chhun S, Harcouet L, Ropert S, Dauphin A, Goldwasser F, Tod M. Validation of an HPLC-UV Method for Sorafenib Determination in Human Plasma and Application to Cancer Patients in Routine Clinical Practice. J Pharm Biomed Anal. 2009; 49:1109–1114. [PubMed: 19278805]
41. Sheu AY, Zhang Z, Omary RA, Larson AC. Invasive Catheterization of the Hepatic Artery for Preclinical Investigation of Liver-Directed Therapies in Rodent Models of Liver Cancer. Am J Transl Res. 2013; 5:269–278. [PubMed: 23634238]
42. Fredenberg S, Wahlgren M, Reslow M, Axelsson A. The Mechanisms of Drug Release in poly (lactic-co-glycolic acid)-based Drug Delivery Systems—a Review. Int J Pharm. 2011; 415:34–52. [PubMed: 21640806]
43. Kamaly N, Yameen B, Wu J, Farokhzad OC. Degradable Controlled-Release Polymers and Polymeric Nanoparticles: Mechanisms of Controlling Drug Release. Chem Rev. 2016; 116:2602–2663. [PubMed: 26854975]
44. Zolnik BS, Burgess DJ. Effect of Acidic pH on PLGA Microsphere Degradation and Release. J Controlled Release. 2007; 122:338–344.
45. Aoi W, Marunaka Y. Importance of pH Homeostasis in Metabolic Health and Diseases: Crucial Role of Membrane Proton Transport. BioMed Res Int. 2014; 2014 No. 598986.
46. Häussinger D, Gerok W, Sies H. Hepatic Role in pH Regulation: Role of the Intercellular Glutamine Cycle. Trends Biochem Sci. 1984; 9:300–302.
47. Liu L, Cao Y, Chen C, Zhang X, McNabola A, Wilkie D, Wilhelm S, Lynch M, Carter C. Sorafenib Blocks the RAF/MEK/ERK Pathway, Inhibits Tumor Angiogenesis, and Induces Tumor Cell Apoptosis in Hepatocellular Carcinoma Model PLC/PRF/5. Cancer Res. 2006; 66:11851–11858. [PubMed: 17178882]
48. Gao GH, Li Y, Lee DS. Environmental pH-sensitive Polymeric Micelles for Cancer Diagnosis and Targeted Therapy. J Controlled Release. 2013; 169:180–184.

49. Lee ES, Gao Z, Bae YH. Recent Progress in Tumor pH Targeting Nanotechnology. J Controlled Release. 2008; 132:164–170.

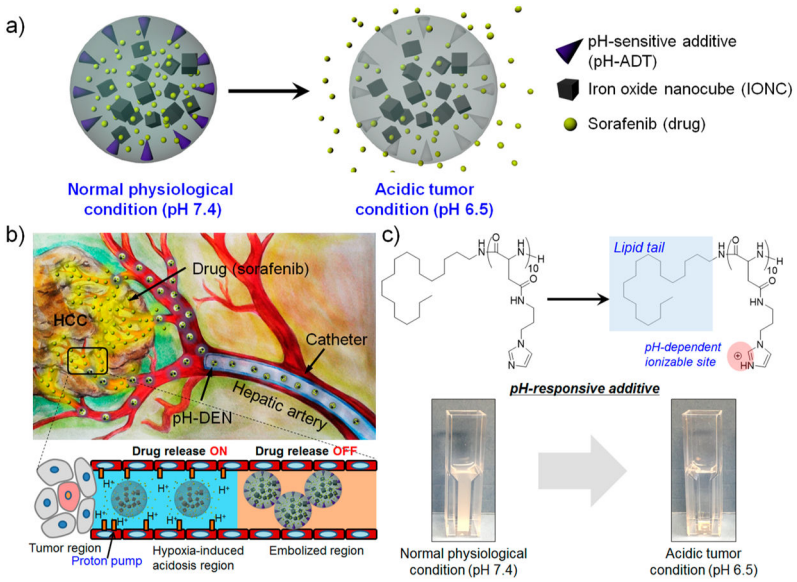

Figure 1.

(a, b) Schematic illustrations of pH-responsive drug-eluting nanocomposites (pH-DENs): (a) acidic pH-triggered drug release behavior and (b) transcatheter hepatic IA delivery of pH-DEN. The drug release of pH-DENs could be triggered by response to the acidic microenvironment caused by embolization-induced hypoxia. (c) Chemical structure of pH-responsive additive (pH-ADT) at different pH values and their pH-dependent phase transition. (Inset) Data for turbidity difference of pH-ADT solutions at pH 7.4 and 6.5.

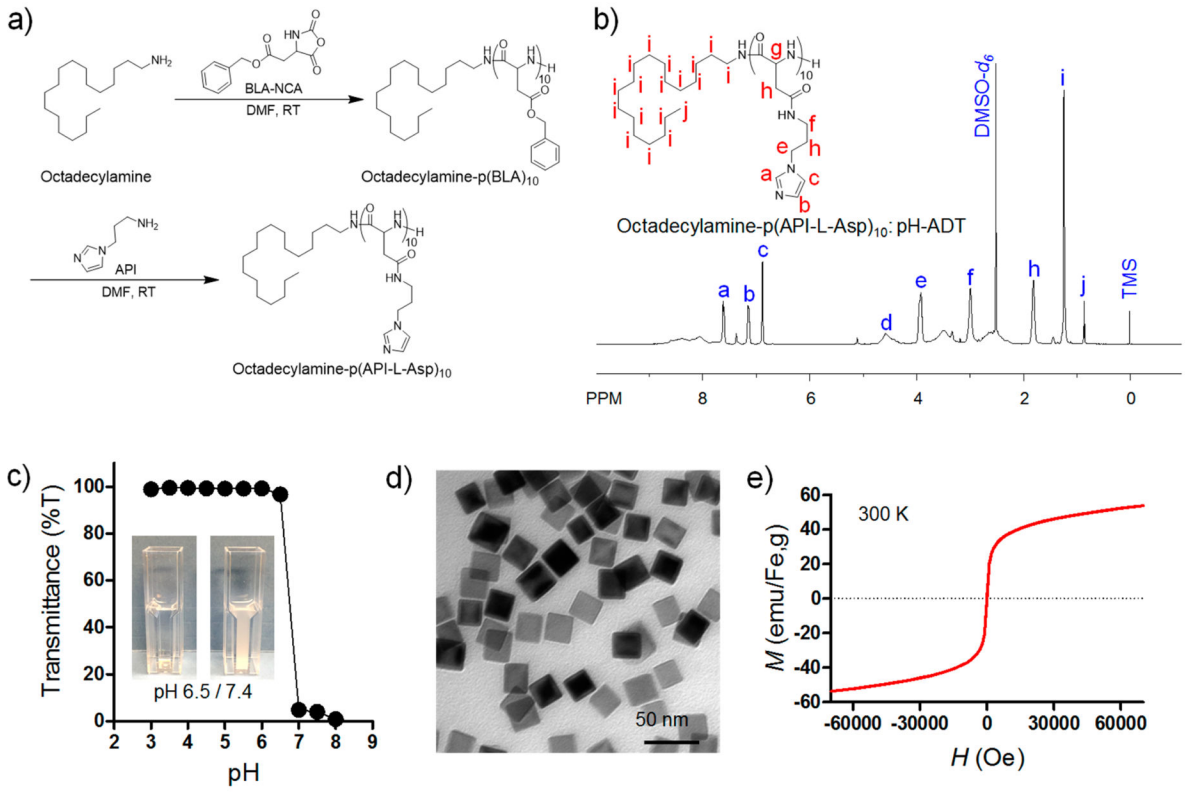

Figure 2.

Synthesis of pH-responsive additive (pH-ADT) and iron oxide nanocubes (IONCs) and their physicochemical characterization. (a) Chemical synthetic route for pH-ADT [octadecylamine–poly(API-L-Asp)$_{10}$]. (b) ^{1}H NMR analysis of pH-ADT in DMSO-d_6. (c) Light transmittance of pH-ADT solution as a function of pH value. (Inset) Data for turbidity difference of pH-ADT solution at pH 6.5 (%T ≈ 97) and 7.4 (%T ≈ 4). (d) TEM image of iron oxide nanocubes (scale bar 50 nm). (e) Field-dependent magnetization curves of IONCs at 300 K.

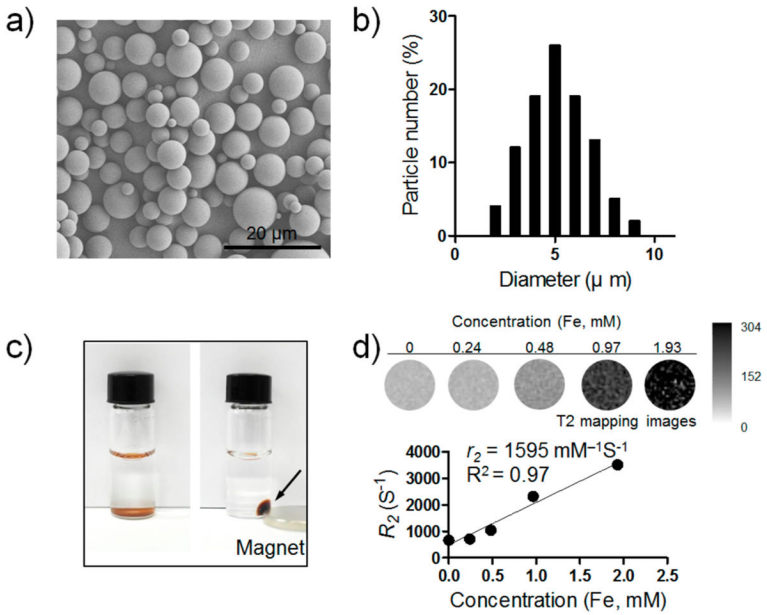

Figure 3.

Physicochemical characterization of pH-DENs. (a) SEM image of pH-DENs (scale bar 20 μm). (b) Size distribution of pH-DENs. (c) Photograph of magnetic separation of pH-DENs [pH-DENs suspensions without (left) or with (right) 500 G magnet]. (d) T_2-weighted MR images and plot of R_2 value of pH-DENs in 1% agar phantoms at various concentrations of iron at 7 T.

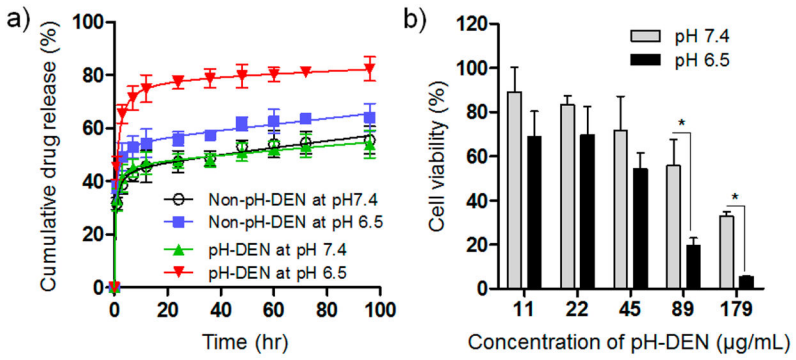

Figure 4.

pH-responsive behavior of pH-DENs. (a) pH-dependent drug release of sorafenib from pH-DEN and non-pH-DEN (control). (b) Cell viability of McA-RH7777 hepatoma cells treated with different concentrations of pH-DEN at pH 7.4 or 6.5 (*$P < 0.01$, $n = 4$).

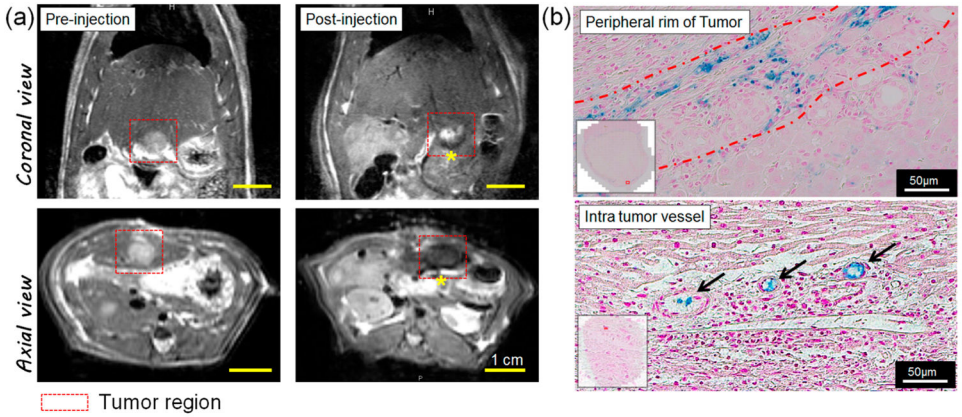

Figure 5.

MRI-monitored hepatic IA transcatheter infusion of pH-DENs in orthotopic HCC rat model. (a) In vivo T_2-weighted MR images acquired before and after transcatheter infusion of pH-DENs. Intrahepatic deposition of pH-DENs is depicted as regions of signal loss within the T_2-weighted images postinfusion (yellow asterisk). (b) Prussian blue staining of treated tumor-bearing liver tissues 24 h post-IA injection. (Top) Peripheral rim and (bottom) intratumor vessels at edge of tumor.

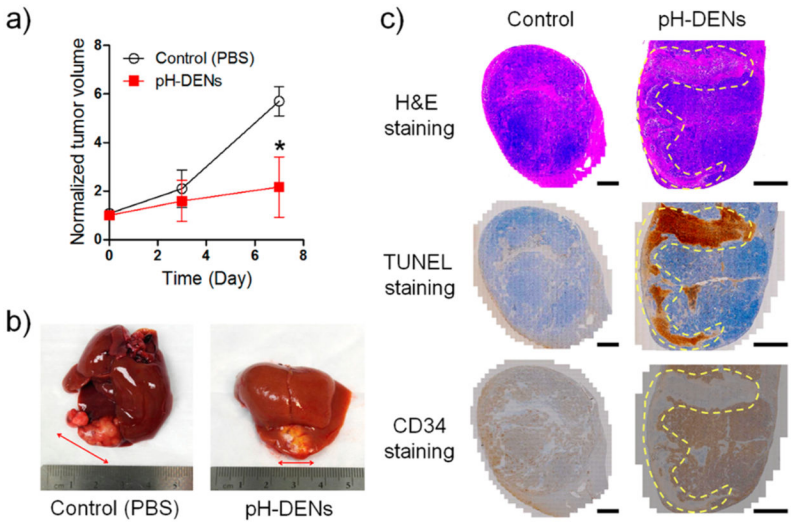

Figure 6.

In vivo tumor growth inhibition following transcatheter infusion of pH-DEN in the orthotopic HCC rat model. (a) Change in normalized tumor volume as a function of time after transcatheter infusion of pH-DEN ($n = 3$, $*P < 0.05$). (b) Representative photograph of extracted tumor-bearing liver from PBS-treated (left) and pH-DEN-treated (right) group. (c) Staining by H/E (top), TUNEL (middle), and CD34 immunohistochemical (IHC) (bottom) methods of tumor tissue sections to assess the efficacy of treatment. The brown color in TUNEL and CD34 staining indicate TUNEL-positive apoptotic cells and microvessels in tumor, respectively (scale bar 2 mm).

Table 1

Quantitative Characterization of pH-DENs and Non-pH-DENs

	feed			IONC		sorafenib	
	pH-ADT[a] (mg)	**IONC[b] (mg)**	**sorafenib[c] (mg)**	**loading efficiency[d] (%)**	**contents[d] (wt %)**	**loading efficiency[e] (%)**	**contents[e] (wt %)**
pH-DENs	10	1.0	20	66.0 ± 4.3	0.66 ± 0.04	73.3 ± 2.5	14.66 ± 0.50
non-pH-DENs		1.0	20	63.2 ± 6.4	0.63 ± 0.06	52.3 ± 4.0	10.47 ± 0.81

[a]Weight of feed pH-ADT per 100 mg of PLGA.

[b]Weight of feed iron oxide nanocubes (IONC) per 100 mg of PLGA.

[c]Weight of feed sorafenib per 100 mg of PLGA.

[d]Encapsulation efficiency = (actual mass of IONC or sorafenib/feed mass of IONC or sorafenib) × 100, as determined by ICPOES.

[e]Loading contents = (actual mass of IONC or sorafenib/actual total mass of NCS) × 100, as determined by HPLC (n = 3).

ACS Appl Mater Interfaces. Author manuscript; available in PMC 2017 May 25.